

Analysis of Schottky-Barrier Millimetric Varactor Doublers

ELIO BAVA, GIAN PAOLO BAVA, ALDO GODONE, AND GIOVANNI RIETTO

Abstract—An analysis of abrupt-junction millimetric varactor doublers using Schottky diodes is performed and numerically implemented to evaluate the conditions of maximum output power. This power level, the efficiency, and the circuit parameters have been derived as a function of the geometrical and physical parameters of the junction. Physical phenomena which allow the application of the model up to the plasma resonance frequency in the epilayer are taken into account. Comparison of available experimental data with the theory developed is reported.

I. INTRODUCTION

IN THE LAST few years the use of Schottky-barrier diodes with micron size junctions has widely increased. The usefulness of these devices has been proved in different fields such as communications, spectroscopy, and frequency metrology.

In the millimetric region, fundamental and harmonic Schottky diode mixers have been studied and developed [1]–[4] with good and reliable performance. Schottky diode varactors have also been used for harmonic generation up to 600 GHz [5],[6] with satisfactory efficiency.

Varactor frequency multipliers have been widely studied for applications up to the microwave region. A comprehensive treatment and an ample review can be found in [7],[8]; whereas closed-form expressions for abrupt-junction diodes are reported in [9]. However, to analyze the behavior of varactor multipliers up to the submillimetric region, one must consider several phenomena such as skin effect, dielectric relaxation, and carrier inertia, which introduce frequency-dependent parameters in the diode model. In this way, the theoretical limitations in the performance at increasing frequencies, taking into account the present technology of GaAs millimetric diodes, can be evaluated.

In this paper, the design of abrupt-junction varactor doublers with maximized output power will be discussed. This goal is imposed by the limited power handling capability of the devices suitable for millimetric frequency operation. Efficiency and matching problems will also be analyzed; a comparison with the available experimental results will be reported in the last part of the work.

II. HIGH-FREQUENCY SCHOTTKY DIODE MODEL

The traditional varactor model [7]–[9] must be modified for operation at high frequencies to incorporate the follow-

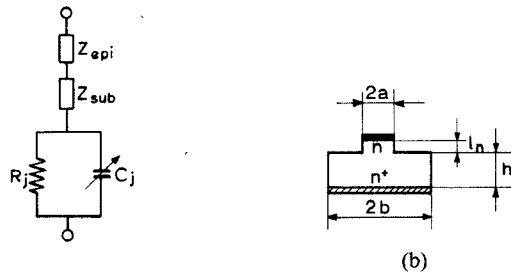


Fig. 1. (a) Schottky diode equivalent circuit. (b) Epitaxial diode geometry.

TABLE I
TYPICAL GEOMETRICAL AND PHYSICAL PARAMETERS OF
n-GaAs SCHOTTKY-BARRIER MILLIMETRIC DIODE

$\Phi_B = 0.85 \text{ V}^a$	Barrier contact potential
$\epsilon_s = 9.59 \times 10^{-11} \text{ F/m}$	Semiconductor permittivity
$n^+ = 2 \times 10^{18} \text{ at/cm}^3$	Substrate carrier concentration
$n = 2 \times 10^{16} \text{ to } 10^{18} \text{ at/cm}^3$	Epilayer carrier concentration
$\frac{m^*}{m_0} = 0.068$	Carrier effective mass
$e = 1.6 \times 10^{-19} \text{ C}$	Electron charge
μ ref. Sze [11]	Carrier mobility
h	Substrate thickness
l	epilayer thickness
$2a$	Junction diameter
$2b$	Substrate diameter
ρ	Epilayer resistivity
$\rho^+ = 1 \times 10^{-3} \Omega^{-1} \text{ cm}^{-1}$	Substrate resistivity
$\omega_{se} = \frac{e}{m^* \mu}$	Epilayer scattering frequency
$\omega_{de} = \frac{1}{\epsilon_s \rho}$	Epilayer dielectric relaxation frequency
ω_s	Substrate scattering frequency
ω_d	Substrate dielectric relaxation frequency

^aFor GaAs, Φ_B is widely independent of the metal used [11, p. 377].

^bIn the numerical computations the effect of ω_d can be neglected.

ing effects:

- 1) skin effect (mainly in the substrate);
- 2) dielectric relaxation (mainly in the epilayer);
- 3) carrier scattering both in the epilayer and in the substrate.

These phenomena have already been taken into account by several authors [4],[5],[10]. The assumed schematic diode structure and its equivalent circuit are shown in Fig. 1, where $Z_{\text{епи}}$ and $Z_{\text{суб}}$ are the epilayer and substrate impedance, respectively, R_j and C_j are the junction resistance and capacitance. Typical values of physical and geometrical parameters for n-GaAs diodes are reported in Table I.

Manuscript received February 27, 1981; revised June 27, 1981. This work was supported by the Consiglio Nazionale delle Ricerche of Italy.

E. Bava, A. Godone, and G. Rietto are with the Istituto Elettrotecnico Nazionale Galileo Ferraris, Turin, Italy.

G. P. Bava is with the Istituto di Elettronica e Telecomunicazioni del Politecnico di Torino, Turin, Italy.

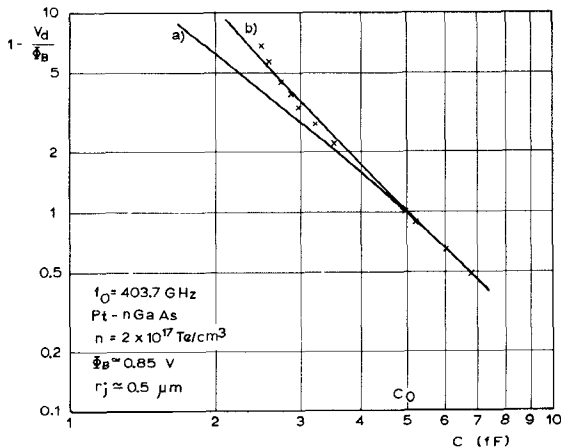


Fig. 2. Junction capacitance versus voltage: x experimental points. (a) C_j for abrupt plane junction. (b) C_j for abrupt spherical junction.

According to [4],[10], the analytical expressions for the electrical parameters of the equivalent circuit (Fig. 1(a)), are as follows:

$$Z_{\text{epi}} = \frac{\rho'}{\pi a^2} \left[\frac{1}{1+j(\omega/\omega_{se})} + j \frac{\omega}{\omega_{de}} \right]^{-1} \quad (1)$$

if the undepleted space-charge region thickness $t \ll a$:

$$Z_{\text{sub}} = \frac{\rho^+}{2\pi\delta} \ln \frac{b}{a} \frac{\sqrt{2j}}{\sqrt{\frac{1}{1+j(\omega/\omega_s)} + j \frac{\omega}{\omega_d}}} + \frac{\rho^+}{4a} \frac{1}{\frac{1}{1+j(\omega/\omega_s)} + j \frac{\omega}{\omega_d}} \quad (2)$$

if $b \gg a$: $R_j \simeq \frac{\eta V_T}{I_s}$, extremely high in varactor operation

$$C_j = \frac{C_{j0}}{(1 - v/\Phi_B)^{\gamma(v)}}. \quad (3)$$

In (1)–(3) we have:

- δ substrate skin depth
- η diode ideality factor
- V_T volt equivalent of temperature
- I_s reverse saturation current
- C_{j0} zero bias junction capacitance
 $= \pi a^2 \sqrt{(e\epsilon_0 n / 2\Phi_B)}$
- v voltage across the junction.

The assumed expression (3) for C_j requires some comments when used at very high frequencies.

1) It is frequency independent (the problem of frequency dependence is theoretically analyzed in [12]), and for high doping levels this assumption is justified.

2) We consider $\gamma = \frac{1}{2}$, that is an ideal, plane, abrupt junction; this approximation is less and less accurate as the junction diameter becomes smaller and consequently the edge effects lead to a spherical structure behavior [13].

Experimental measurements of C_j for a 2-μm diameter diode, carried out at 403.7 GHz [14], which demonstrate the preceding point, are shown in Fig. 2. Curve (a) refers to the model of an ideal plane abrupt junction. Curve (b)

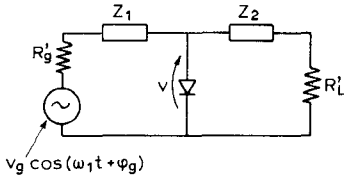


Fig. 3. Frequency doubler circuit model.

refers to a spherical model with 1-μm diameter. Even if the experimental points are better fitted by curve (b), curve (a) also can be considered a satisfactory approximation. Moreover the experimental value of C_{j0} is in good agreement with its low-frequency estimate.

The power handling capability of a varactor multiplier is limited by the breakdown voltage V_{BR} . In the already accepted hypothesis of an abrupt plane junction we have [11] for the avalanche breakdown:

$$V_{BR} = 60 \left(\frac{Eg}{1.1} \right)^{3/2} \left(\frac{n}{10^{16}} \right)^{-3/4} [\text{V}] \quad (4)$$

where Eg is the band energy gap in electronvolts (for GaAs $Eg = 1.43$ eV) and n in cm^{-3} .

III. MILLIMETRIC VARACTOR DOUBLER ANALYSIS

The frequency doubler circuit model adopted is shown in Fig. 3 with the assumptions discussed in [9] and in particular:

1) Z_{epi} and Z_{sub} are included in the impedances Z_1 ($Z_1 = R_1 + jX_1$) and Z_2 ($Z_2 = R_2 + jX_2$) (Fig. 3) at the respective frequencies;

2) Z_1 and Z_2 allow the current to flow only at the fundamental (ω_1) and second-harmonic ($\omega_2 = 2\omega_1$) frequencies, respectively.

As a consequence the varactor charge can be written

$$q = q_0 + q_1 \sin(\omega_1 t + \varphi_1) + q_2 \sin(\omega_2 t + \varphi_2) \quad (5)$$

and (3) can be readjusted as a relation between charge and voltage:

$$v(q) = \Phi_B - mq^2, \quad m = \frac{1}{4\Phi_B C_{j0}}. \quad (6)$$

By using (5) and (6), the loop equations for the network of Fig. 3 become [9]

$$\begin{aligned} v_g \cos(\varphi_1 - \varphi_g) &= \omega_1 q_1 \left(R_g - \frac{mq_2 \cos \varphi_0}{\omega_1} \right) \\ v_g \sin(\varphi_1 - \varphi_g) &= -X_1 \omega_1 q_1 - 2mq_0 q_1 + mq_1 q_2 \sin \varphi_0 \\ 0 &= R_L \omega_2 q_2 + \frac{m}{2} q_1^2 \cos \varphi_0 \\ 0 &= -X_2 \omega_2 q_2 + \frac{m}{2} q_1^2 \sin \varphi_0 - 2mq_0 q_2 \end{aligned} \quad (7)$$

where

$$\varphi_0 = \varphi_2 - 2\varphi_1$$

$$R_g = R'_g + R_1$$

$$R_L = R'_L + R_2.$$

The limited power handling capability of millimetric

varactors suggests the circuit design (in our model the choice of R_1, R_2, X_1, X_2) so as to maximize the output power with the maximum capacitance swing:

$$-\sqrt{\frac{V_{BR} + \Phi_B}{m}} = q_m < q < 0. \quad (8)$$

Moreover the circuit matching implies [8], [9] $\varphi_0 = \pi$ and $R'_g = R_1 + R_{in}$ where $R_{in} = mq_2/\omega_1$. These conditions, by using (5), (7), and (8), lead to

$$\begin{cases} q_2 = \frac{|q_m|}{2\sqrt{1-\cos^2 x}(q_1/q_2 - 2\cos x)} \\ \cos x = -\frac{4}{1 + \sqrt{1 + 32(q_2/q_1)^2}} \frac{q_2}{q_1} \end{cases} \quad (9)$$

$$q_1^2 = \frac{4\omega_1 R_2}{m} q_2 + \frac{2P_0}{m\omega_1} \frac{1}{q_2} \quad (10)$$

where the output power $P_0 = \frac{1}{2}(\omega_2 q_2)^2 R'_L$. In the plane $q_1 - q_2$, (9) gives the curve representing the breakdown limit and (10) the family of constant output power curves. Examples of similar graphical representations can be found in [7, pp. 326 and 576]. The mathematical condition of maximum output power is found by imposing the geometrical tangency between (9) and (10).

The following fourth-degree equation is obtained:

$$(4+k)u^4 - 6(2+k)u^3 + (13+12k)u^2 - 2(3+4k)u + 1 = 0 \quad (11)$$

where

$$k = \left(\frac{2\omega_1 R_2}{mq_m} \right)^2$$

and

$$u = 2\cos^2 x.$$

Equation (11) can be easily solved for instance by using Newton's iteration method. After solving (11), q_1 , q_2 , and $P_{0\max}$ are found from (9) and (10). The other quantities of interest in the multiplier design are obtained from (7), and are reported in the following.

Efficiency

$$\eta = \frac{u}{2(1-u)^2} \frac{R'_L}{R'_g}$$

Generator internal resistance

$$R'_g = R_1 + \frac{mq_2}{\omega_1}$$

Load resistance

$$R'_L = \frac{P_0}{2\omega_1^2 q_2^2}$$

Input and output reactances

$$X_1 = \frac{2m}{\omega_1} \sqrt{1 - \frac{u}{2}} (q_1 + q_2 \sqrt{2u})$$

$$X_2 = X_1/2.$$

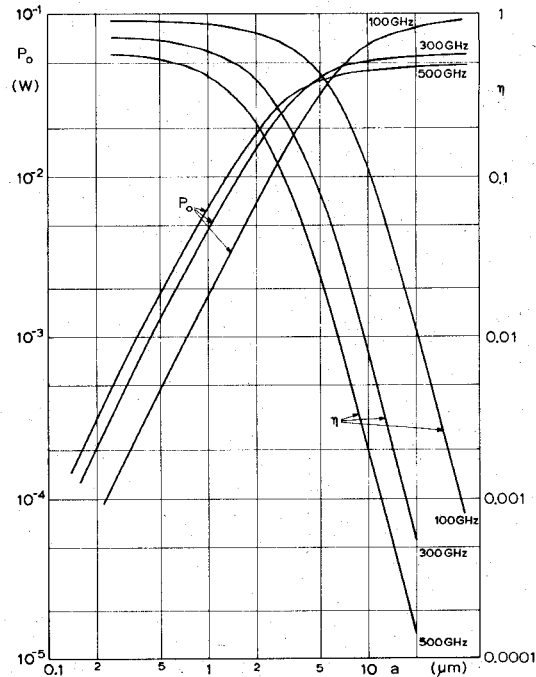


Fig. 4. Maximum output power and efficiency versus junction radius for n-GaAs diodes.

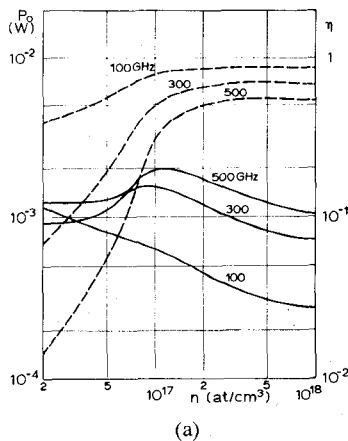
IV. NUMERICAL RESULTS AND COMPARISON WITH EXPERIMENTS

Following the expressions reported in the preceding section a numerical computation of the performance of Schottky-barrier varactor frequency doublers has been carried out. The material and geometrical parameters are those already given in Table I. We have considered as independent variables: among the geometrical dimensions the junction radius and among the physical parameters the epilayer doping.¹ The frequency range under examination is 50–500 GHz for the input signal frequency. In the evaluation of (1), strictly speaking the undepleted region thickness t is time dependent, but in our computation t has been assumed fixed and equal to the epilayer thickness l_n . As a consequence a slight overestimation of the diode losses turns out; moreover the nonlinear resistance contribution to the multiplication process is neglected.

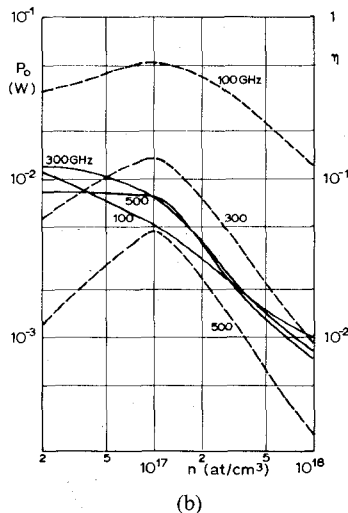
The maximum output power P_0 and the efficiency η for a Pt-n-GaAs junction with $n = 2 \times 10^{17}/\text{cm}^3$ are shown as a function of the radius a in Fig. 4. For increasing a (junction radius) the output power increases owing to a larger charge excursion and the efficiency decreases (as a consequence of the unfavorable resistance–capacitance partition) [9].

For small values of a the output power increases with frequency; this is due to the dominant capacitive effect, typical of low values of a , enhanced for increasing frequency. For high values of a the resistive losses increase and, due to the frequency dependence of R_2 , a higher power is obtained at lower frequencies. Asymptotically, as $a \rightarrow \infty$, by using the expressions of the preceding section,

¹For b/a and n^+ (Table I) standard values have been assumed.



(a)



(b)

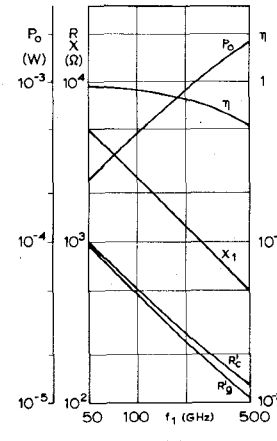
Fig. 5. Maximum output power (continuous lines) and efficiency (dashed lines) versus epilayer doping for: (a) $a=0.5 \mu\text{m}$; (b) $a=5 \mu\text{m}$.

we have

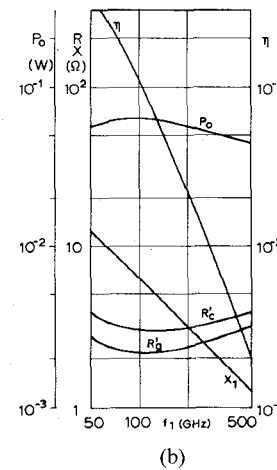
$$P_{0\max} \rightarrow \frac{1}{2^9} \frac{(V_{BR} + \Phi_B)^2}{R_2}$$

The influence of the epilayer doping n on the output power and efficiency is shown in Fig. 5(a) ($a=0.5 \mu\text{m}$) and 5(b) ($a=5 \mu\text{m}$). From the figures it turns out that the maximum of the efficiency is reached at lower values of n when the junction radius increases. At small a and high input frequencies, the effects of the resistive losses and of the plasma resonance give rise to a maximum of output power versus n .

The frequency dependence of efficiency, maximum output power, load and generator resistance and tuning reactances are shown in Fig. 6(a) and (b) for two different values of the contact radius and for the same epilayer doping as used in Fig. 4. The results reported in Fig. 6 show that it is possible to obtain rather high power levels by increasing the junction diameter, but this is paid with a low efficiency; moreover the practical achievement of these conditions implies difficulties in building the matching circuits owing to the small values of reactances and resistances.



(a)



(b)

Fig. 6. Maximum output power, efficiency, input and output resistances and reactances versus input frequency for: (a) $a=0.5 \mu\text{m}$; (b) $a=10 \mu\text{m}$.

TABLE II
COMPARISON OF EXPERIMENTAL AND THEORETICAL RESULTS
FOR MILLIMETRIC VARACTOR DOUBLERS

$\omega_1/2\pi$ (GHz)	P_o (mW) exper.	P_o (mW) this theory	η % exper.	η % this theory	Reference
100	18	72	12	59	[5]
150	0.4	1.6	10	75	[6]
150	0.4	1.3	10	75	
150	5	6.1	9.3	60.7	[15]
100	0.28	1.2	(*)	86	present work

(*) the efficiency value obtained is meaningless, since no matching has been tried on the commercial mount used.

The results of the theoretical analysis presented in this paper can be compared with some experimental data found in the literature and with some measurements carried out by the authors. Table II summarizes this comparison as regards efficiency and output power. The discrepancies between theoretical and experimental values can well be attributed to the experimental difficulties in realizing the

matching for maximum output power, additional losses in the tuning circuits as well as to the measurement inaccuracies and uncertainties in the geometrical and physical diode parameters. Moreover the assumed diode and circuit models might not correspond accurately to the devices used (see, for instance, Fig. 2).

V. CONCLUSIONS

A theoretical treatment of frequency doublers using Schottky-barrier abrupt-junction varactor diodes has been presented. The model includes physical phenomena so that its application holds up to approximately the plasma resonance frequency in the epilayer. Conditions for maximum output power have been derived depending on the diode parameters; also in the present case the maximum efficiency condition is not too far from the maximum output power [7].

Beside the limitations of the circuit model used in Section III, the analysis has been developed with the following hypotheses: abrupt plane junction, voltage-independent epilayer resistances.

Numerical computations of output power, efficiency and circuit parameters have been reported in Section IV for n-GaAs Schottky diodes, neglecting external circuit losses. Some comparisons with experimental data are reported.

REFERENCES

- [1] H. R. Fetterman, P. E. Tannenwald, B. J. Clifton, C. D. Parker, W. D. Fitzgerald, and N. R. Erickson, "Far-IR heterodyne radiometric measurements with quasioptical Schottky diode mixers," *Appl. Phys. Lett.*, vol. 32, no. 2, pp. 151-154, July 15, 1978.
- [2] E. R. Carlson, M. V. Schneider, and T. F. McMaster, "Subharmonically pumped millimeter-wave mixers," *IEEE Trans. Microwave Theory Tech.*, vol. MTT-26, pp. 706-715, Oct. 1978.
- [3] D. N. Held and A. R. Kerr, "Conversion loss and noise of microwave and millimeter-wave mixers—Part 1: Theory; Part 2: Experiment," *IEEE Trans. Microwave Theory Tech.*, vol. MTT-26, pp. 49-61, Feb. 1978.
- [4] W. M. Kelly and G. T. Wrixon, "Conversion losses in Schottky barrier diode mixers in the submillimeter region," *IEEE Trans. Microwave Theory Tech.*, vol. MTT-27, pp. 665-672, July 1979.
- [5] J. A. Calviello, "Advanced devices and components for the millimeter and submillimeter systems," *IEEE Trans. Electron Devices*, vol. ED-26, pp. 1273-1281, Sept. 1979.
- [6] T. Takada and M. Ohmori, "Frequency triplers and quadruplers with GaAs Schottky-barrier diodes at 450 and 600 GHz," *IEEE Trans. Microwave Theory Tech.*, vol. MTT-27, pp. 519-523, May 1979.
- [7] P. Penfield, and R. P. Rafuse, *Varactor Applications*. Cambridge, MA: M.I.T. Press, 1962.
- [8] J. O. Scanlan, "Analysis of varactor harmonic generators," in *Advances in Microwaves*, L. Young, Ed. New York: Academic Press, vol. 2.
- [9] E. Bava, G. P. Bava, A. Godone, and G. Rietto, "Analysis of varactor frequency multipliers: non linear behavior and hysteresis phenomena," *IEEE Trans. Microwave Theory Tech.*, vol. MTT-27, pp. 141-147, Feb. 1979.
- [10] K. S. Champlin and G. Eisenstein, "Cutoff frequency of submillimeter Schottky-barrier diodes," *IEEE Trans. Microwave Theory Tech.*, vol. MTT-26, pp. 31-34, Jan. 1978.
- [11] S. M. Sze, *Physics of Semiconductor Devices*. New York: Wiley Interscience, 1969.
- [12] K. Hesse and H. Strack, "On the frequency dependence of GaAs Schottky-barrier capacitances," *Solid State Electron.*, vol. 15, pp. 767-774, 1972.
- [13] T. P. Lee and S. M. Sze, "Depletion layer capacitance of cylindrical and spherical p-n junctions," *Solid State Electron.*, vol. 10, pp. 1105-1108, 1967.
- [14] A. Godone, E. Bava, and A. De Marchi, "FIR laser modulation by an external variable reactance," *IEEE Trans. Instrum. Meas.*, vol. IM-29, pp. 277-283, Dec. 1980.
- [15] T. Takada, T. Makimura, and M. Ohmori, "Hybrid integrated frequency doublers and triplers to 300 and 450 GHz," *IEEE Trans. Microwave Theory Tech.*, vol. MTT-28, pp. 966-973, Sept. 1980.

+

Elio Bava was born in 1940. He received the degree in electronic engineering from the Politecnico di Torino, Turin, Italy, in 1964.

In 1966 he joined the Istituto Elettrotecnico Nazionale "Galileo Ferraris", Turin, where, for a few years, he was involved in satellite communication research and microwave metrology. Afterwards he was interested in frequency multiplication from the UHF to the microwave region. At present his activity concerns frequency synthesis in the millimeter and the submillimeter regions and characterization of frequency stability of far-infrared lasers.

+

Gian Paolo Bava was born in 1937. He received the degree in electrical engineering from the Politecnico di Torino, Turin, Italy, in 1961.

Since 1961 he has been engaged in research at the Istituto di Elettronica e Telecomunicazioni (Politecnico di Torino) and at the Istituto Elettrotecnico Nazionale Galileo Ferraris (Turin). His research activities have been primarily concerned with TWT linearization, microwave transistor amplifiers, frequency multipliers, integrated optics. At present he also holds the rank of Professor of Microwave Techniques at the Politecnico di Torino.

+

Aldo Godone was born in Turin, Italy, in 1949. He received the Dr. Ing. degree in electronic engineering from the Politecnico of Torino, Turin, Italy, in 1974.

Since 1974 he has been in the microwave group of the Istituto Elettrotecnico Nazionale Galileo Ferraris of Turin, Italy. His research activity is primarily concerned with frequency multiplication by harmonic generation in the microwave and in the submillimeter regions and in infrared laser stabilization for metrological purposes.

+

Giovanni Rietto was born in Moncalieri, Italy, on March 8, 1935. He received the degree in electrical engineering from the Politecnico di Torino, Turin, Italy, in 1960.

Since 1962, he has been engaged in research in the radio department of the Istituto Elettrotecnico Nazionale Galileo Ferraris, Turin, Italy. He has worked on spurious radiation measurements in connection with Special Committee on Radio Interference (CISPR) studies, and, since 1965, he has been concerned with high accuracy microwave metrology. In these last years, he has been increasingly involved in the solution of electromagnetic and electronic problems with digital computers.